Revista Brasileira de Farmacognosia (2026) 36:47
https://doi.org/10.1007/s43450-026-00759-8

ORIGINAL ARTICLE

Exploring Anatomical and Chemical Markers to Characterize and Differentiate Among *Bidens* Species

Carolina Sabedotti[1] · Isabella da Silveira[2] · Izabel Pietczak Migacz[1] · Luiza Stolz Cruz[3] · Ana Carolina Terso Ventura[1] · Paulo Vitor Farago[1,2] · Claudio Augusto Mondin[4] · Vijayasankar Raman[5] · Edy Sousa de Brito[6] · Paulo Riceli Vasconcelos Ribeiro[7] · Flávio Luís Beltrame[1] · Jane Manfron[1,2]

Received: 12 December 2025 / Accepted: 25 March 2026

Abstract

Bidens pilosa L., *Bidens alba* (L.) DC., and *Bidens subalternans* DC., Asteraceae, are often misidentified because of their morphological similarities. The present study provides a comparative analysis of the morpho-anatomical characteristics, histochemical, and chemical fingerprints obtained by liquid chromatography mass spectrometry for these three species. Light microscopy, field emission scanning electron microscopy, and energy-dispersive X-ray spectroscopy were used to characterize diagnostic structures. Histochemical assays and LC-MS were applied to obtain chemical information from leaf, stem, and root extracts, and multivariate chemometrics including principal component analysis were used to classify the datasets. The morpho-anatomical and histochemical analysis allowed the identification and differentiation of the three species; also, the LC-MS analysis revealed that the main compounds in *Bidens* extracts are phenolics, and using chemometrics methods was possible to discriminate by species and plant parts. Together, these complementary approaches provide a robust basis for distinguishing closely related *Bidens* species and support more reliable pharmacognostic identification.

Keywords Chemotaxonomy · Herbals · Micromorphology · Pharmacobotany · Quality control · Species authentication

Introduction

The genus *Bidens* L., Asteraceae, is cosmopolitan and comprises about 223 species (POWO 2025). Species of *Bidens* are commonly called as Spanish needles, beggar's ticks, devil's needles, cobbler's pegs, broom stick, pitchforks, burmarigold, black Jack, and farmers' friends in the USA (Bartolome et al. 2013); "cadillo rocero" in Venezuela; "amorseco" and "pirca" in Peru; "pinyin" and "jin zhan yin pan" in China; and "pico-pico," "picão", picão-preto, carrapicho, piolho-de-padre, picão-do-campo, erva-picão, and fura-capa in Brazil (Gilbert et al. 2013; Bringel et al. 2025).

Nineteen species are native to Brazil, and *Bidens pilosa* L., *B. alba* (L.) DC., and *Bidens subalternans* DC. share the same common name and are morphologically similar (Grombone-Guaratini et al. 2004; Lorenzi and Matos 2008), creating the "*Bidens pilosa* complex". The circumscription of this complex may vary across regions; in southeastern Brazil, this complex has been treated as comprising *B. pilosa*, *B. alba*, and *B. subalternans*, three closely related taxa with extensive overlap in diagnostic traits (Grombone-Guaratini et al. 2005, 2006). Traditional delimitation within

Carolina Sabedotti and Isabella da Silveira contributed equally to this work.

✉ Flávio Luís Beltrame
flaviobeltra@uepg.br

✉ Jane Manfron
jane@uepg.br

1 Programa de Pós-graduação em Ciências Farmacêuticas, Universidade Estadual de Ponta Grossa, Ponta Grossa, Paraná, Brazil

2 Programa de Pós-gradução em Ciências da Saúde, Universidade Estadual de Ponta Grossa, Ponta Grossa, Paraná, Brazil

3 Departamento de Ciências Farmacêuticas, Universidade Estadual do Centro-Oeste, Guarapuava, Paraná, Brazil

4 Instituto Conectar Ambiental, Higienópolis, Porto Alegre, Rio Grande do Sul, Brazil

5 Department of Agriculture, District of Columbia, National Identification Services, Washington, USA

6 Programa de Pós-graduação em Engenharia Química, Universidade Federal do Ceará, Fortaleza, Ceará, Brazil

7 Embrapa Agroindústria Tropical, Fortaleza, Ceará, Brazil

Published online: 30 April 2026

the complex relies mainly on morphological characters, especially capitulum traits and achene features including the pappus awns; however, these may vary within species and across populations, making identifications imprecise and often controversial when based solely on external morphology (Grombone-Guaratini et al. 2004). Cytogenetic evidence further supports the complexity and provides an additional discriminant line of evidence, since *B. pilosa* has been reported with $2n = 72$, whereas *B. subalternans* and *B. alba* have $2n = 48$, indicating that polyploidy and cytotype differences contribute to the taxonomic difficulty and can assist in species separation (Grombone-Guaratini et al. 2006).

Moreover, in traditional medicinal systems, these three species are used interchangeably as anti-inflammatory, antiseptic, hepatoprotective, anti-hypokinetic, blood pressure reducer, antiulcerogenic, and to treat digestive disorders, diabetes, cancer, jaundice, malaria, angina, influenza, colds, pains, fevers, and edema. These biological properties are attributed to the presence of secondary metabolites such as phenylpropanoids, terpenes, and polyacetylenes, but mainly the phenolic compounds such as flavonoids and phenolic acids (Ortega et al. 2000; Grombone-Guaratini et al. 2005; Lans 2006; Ong et al. 2008; Bartolome et al. 2013; Borges et al. 2013; Silva et al. 2013; Gbashi et al. 2017).

Several studies in Asteraceae have shown that combining diagnostic morpho-anatomical evidence with chemical fingerprinting approaches, including HPTLC and high-resolution LC-MS-based profiling, improves species authentication and strengthens the quality control of botanical raw materials (Antunes et al. 2024; Gempo et al. 2024). In *Bidens*, pharmacobotanical studies have stated useful anatomical and histochemical markers for *B. pilosa*, including epidermal and trichome traits and the localization of phenolic constituents (Duarte and Estelita 1999; Sá et al. 2017). Complementarily, HPLC, LC-MS chemical fingerprinting, and feature-based profiling combined with chemometrics have been applied to characterize *B. pilosa* extracts and discriminate plant organs (Chiang et al. 2004; Cortés-Rojas et al. 2013; Chagas-Paula et al. 2015; Ramabulana et al. 2020).

Thus, the study aimed to compare the morpho-anatomical and chemical profiles of the three *Bidens* species using a combination of morphology, microscopy, micromorphology, and LC-MS techniques to provide a robust background for accurate identification and differentiation of the species.

Materials and Methods

Plant Material

Five individual plants per species (*B. alba*, *B. pilosa*, and *B. subalternans*) were collected ($n = 5$ per species; total $n = 15$). *Bidens pilosa* specimens were collected at Fazenda Escola Capão da Onça (latitude 25° 5′ 43″S and longitude 50° 3′ 26″W) in Ponta Grossa, PR, Brazil. Specimens of *B. subalternans* and *B. alba* were collected at Ponta Grossa State University (latitude 25° 5′ 23″S and longitude 50° 6′ 23″W, and latitude 25° 5′ 23″S and longitude 50° 6′ 23″W, respectively), Ponta Grossa, PR, Brazil. All three species were collected in November 2021, identified by Claudio A. Mondin and the herbarium voucher specimens were deposited in the State University of Ponta Grossa Herbarium (HUPG), under the numbers *Bidens pilosa* (22498), *Bidens subalternans* (21262), and *Bidens alba* (22499).

Optical Microscopy Procedure

Fresh samples from healthy and intact mature leaves, stems, and roots of *B. pilosa*, *B. alba*, and *B. subalternans* were fixed in formalin-acetic acid-alcohol (FAA70) for 3 days (Johansen 1940), washed in distilled water, and stored in 70% ethanol solution (v/v) (Berlyn and Miksche 1976). Leaves, stems, and roots were free-hand sectioned with razors in transversal and longitudinal directions. The sections were stained using astra blue and basic fuchsin (Roeser 1972) and mounted in a drop of 50% glycerin (Berlyn and Miksche 1976) on glass slides, covered with a coverslip, and sealed with transparent nail polish. For the analysis of epidermal surfaces, small sections of the leaves were washed and then treated with hypochlorite solution (5%) until translucent. The materials were then washed in distilled water and neutralized in an acetic acid solution (5%). Later, the sections were washed again with distilled water and stained with safranin (Fuchs 1963) and mounted as described above.

Micro-measurements

Quantitative studies of stomata were performed by taking 20 measurements from multiple leaf specimens. Stomatal index (SI) was calculated using the following formula, wherein S = number of stomata per unit area, and E = number of epidermal cells (including trichomes) in the same unit area. The length and width of stomata were measured from 20 stomata at different locations on the leaf blade for each species to determine the average stomatal size.

Field Emission Scanning Electron Microscopy

For the field emission scanning electron microscopy (FESEM) analyses, the FAA-fixed samples were dehydrated by passing through increasing concentrations of ethanol in water (30, 50, 70, 95, and 100%) and dried in a Leica EM CPD300 critical point dryer (Leica Microsystems, Wetzlar, Germany) using liquid CO_2 as a transitional fluid. The dried samples were coated with gold using a Quorum SC7620 sputter coater (Quorum Technologies Ltd., Kent, UK).

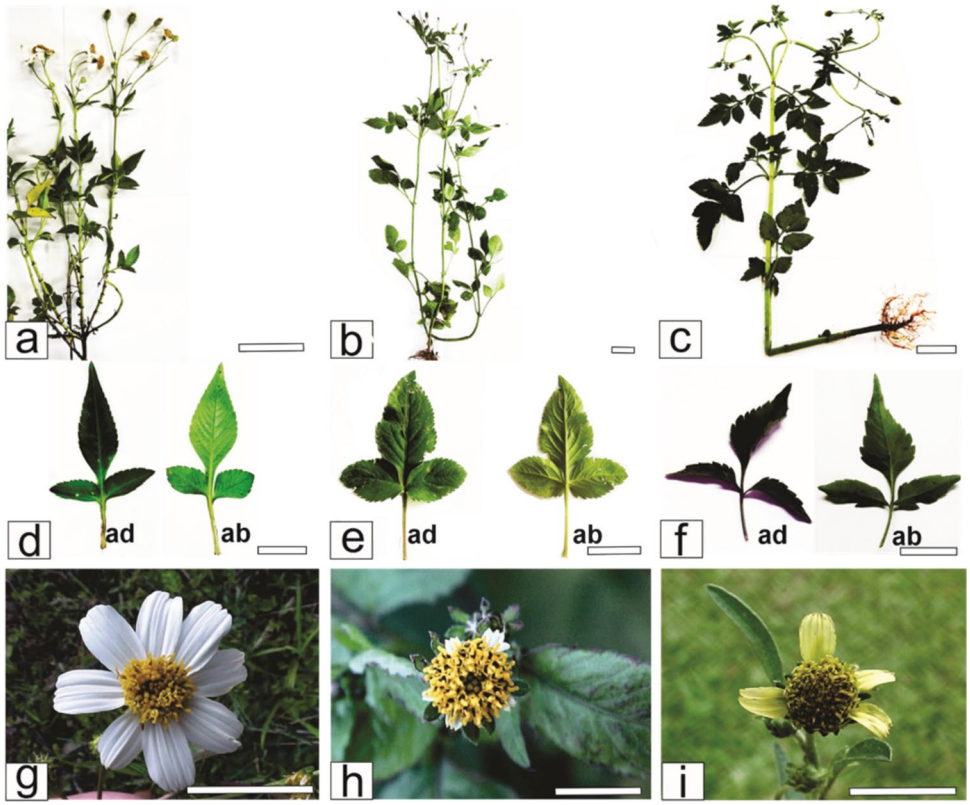

Fig. 1 Morphology of *Bidens* species. **a**, **d**, **g** *Bidens alba*; **b**, **e**, **h** *Bidens pilosa*; **c**, **f**, **i** *Bidens subalternans* (ad, adaxial side; ab, abaxial side). Scale bar: **a**–**c**, **e**, **g** = 5 cm; **d** = 1 cm; **f**, **h**, **i** = 2 cm

Electron micrographs were prepared using a Tescan Mira3 field emission SEM in high vacuum mode with an accelerating voltage of 15 kV. This procedure was performed at the multiuser laboratory (C-Labmu) in the State University of Ponta Grossa.

Energy-Dispersive X-ray Spectroscopy

Energy-dispersive X-ray spectroscopy (EDS) analyses were performed during FESEM observation to characterize the chemical composition of the crystals. Measurements were acquired from crystals as well as from neighboring cells devoid of crystals, which served as internal controls. The analyses were carried out using an EDS detector combined with a FESEM, operated at 15 kV accelerating voltage. All procedures were conducted at the Multiuser Laboratory Complex (C-Labmu), State University of Ponta Grossa.

Histochemical Tests

The FAA-fixed leaves, stems, and roots of *B. pilosa*, *B. alba*, and *B. subalternans* were subjected to histochemical tests. After fixation, samples were transferred to 70% ethanol and stored until sectioning. Free-hand cross-sections were prepared and subjected to histochemical reactions. Staining reactions were performed immediately after sectioning and interpreted qualitatively as *in situ* localization indicators, not for quantitative inference. Because FAA fixation and subsequent storage in ethanol may influence the detectability of readily extractable constituents, especially lipophilic substances and some phenolics, the histochemical results were interpreted conservatively. The sections of the plant materials were tested with standard reagents, such as Sudan III for lipophilic substances (Foster 1949), iodine solution for starch (Berlyn and Miksche 1976), phloroglucinol/HCl to detect lignified components (Sass 1951), potassium dichromate 10% (Gabe 1968), and ferric chloride 2% for phenolic compounds (Johansen 1940). Appropriate controls were processed in parallel under identical conditions.

Extract Preparation and LC-MS Analysis

The samples of roots, stems, and leaves were dried separately in a circulating oven. The extracts were obtained in a Soxhlet extractor using 750 ml of ethanol 96° GL. UPLC/QTOF analyses were performed in a Waters® Ultra Performance Liquid Chromatography comprised of the following modular components: binary pump, a vacuum solvent micro degasser, an auto sampler, a thermostatically controlled column compartment, and coupled to a Xevo Waters® Mass Spectrometer. Chromatographic separation was achieved using a BEH C_{18} (1.7 µm, 2.1 × 100 mm) reversed-phase column. The mobile phase consisted of 0.1% formic acid in water (v/v) (A) and 0.01% formic acid in methanol (v/v)

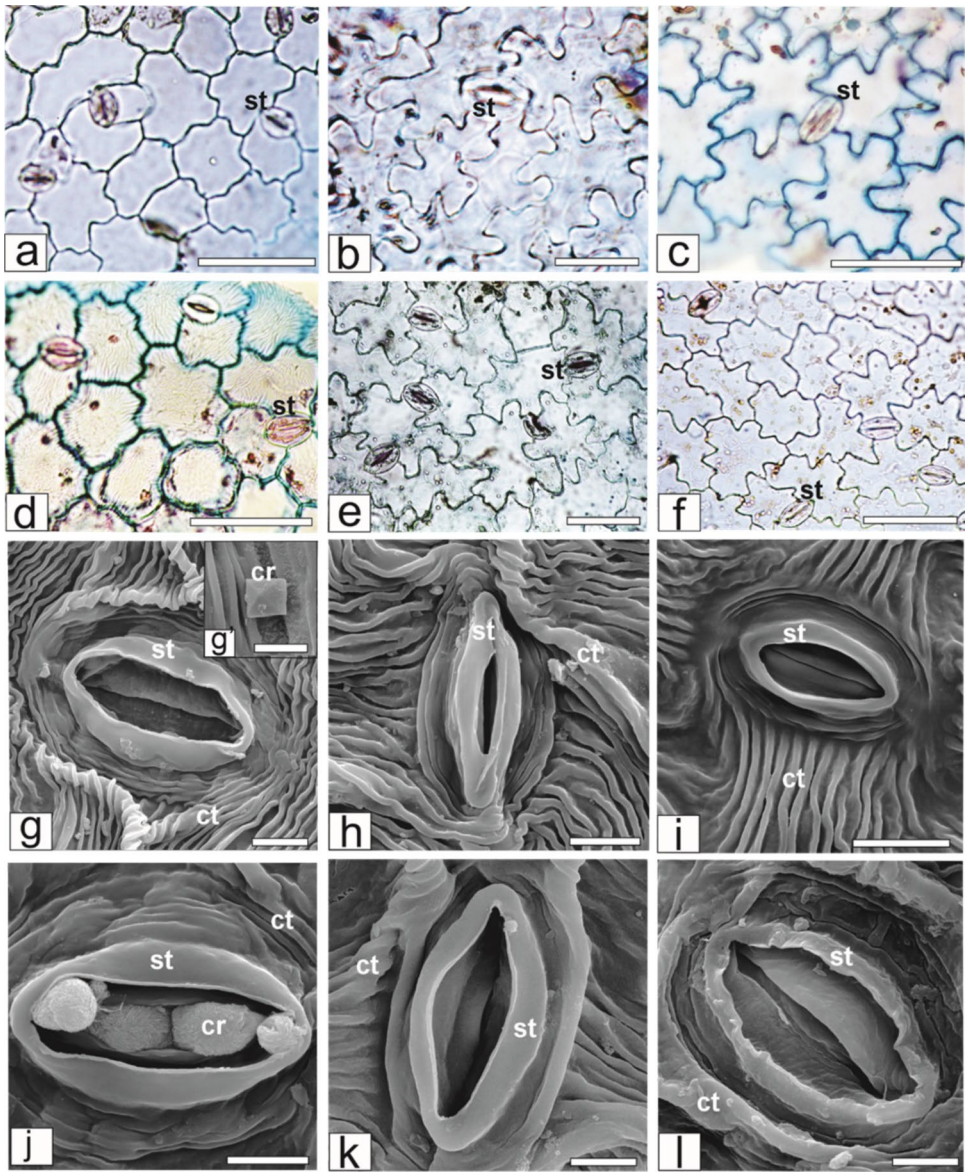

Fig. 2 Leaf epidermis in *Bidens* — frontal view (light microscopy: **a–f** (stained in toluidine blue); scanning electron microscopy: g–l). *B. alba* **a, d, g, g′, j**, *B. pilosa* **b, e, h, k**, *B. subalternans* **c, f, i, l**. Adaxial side **a–c, g–i**, abaxial side **d–f, j–l** (ct, cuticle; cr, crystal; st, stomata). Scale bar: a–f = 50 µm, g–l = 5 µm, g′ = 3 µm

(B) as a binary mobile phase. A gradient elution program was used, starting at 5% B, reaching 100% B over 12 min, holding for 3 min, and then returning to initial conditions within 16 min. The flow rate was 0.3 ml/min, the injection volume was 4 µl, and the column temperature was maintained at 30 °C. The mass spectrometer, operating in negative ion mode, was equipped with an ESI source, and collision energy and cone voltage were set at 40 V each. Accurate mass measurements were obtained by means of ion correction techniques using reference masses at *m/z* 112.9856 (deprotonated trifluoroacetic acid-TFA). The masses were investigated based on MONA (Mass Bank of North America —https://www.massbank.us/and some articles published in the literature (Chiang et al. 2004; Safer et al. 2011; Saltos et al. 2015; Chen et al. 2016; Lusa et al. 2016; Khoza et al. 2016; Gbashi et al. 2017; Machinski et al. 2024).

Multivariate and Univariate Statistical Analysis

The LC-MS chromatograms (range 2 to 8 min) were pre-processed using Masslynx version 4.1. The dataset (27 × 2108) was imported for Matlab, version 2020a, and Icoshift was used for alignment. The singular value decomposition algorithm was used for PCA after smoothing, baseline correction, and mean-centered processing applied over the variables. Specific compound data were evaluated by the analysis of variance and the Tukey test ($p < 0.05$), and the Levene test was applied to verify the variance homogeneity.

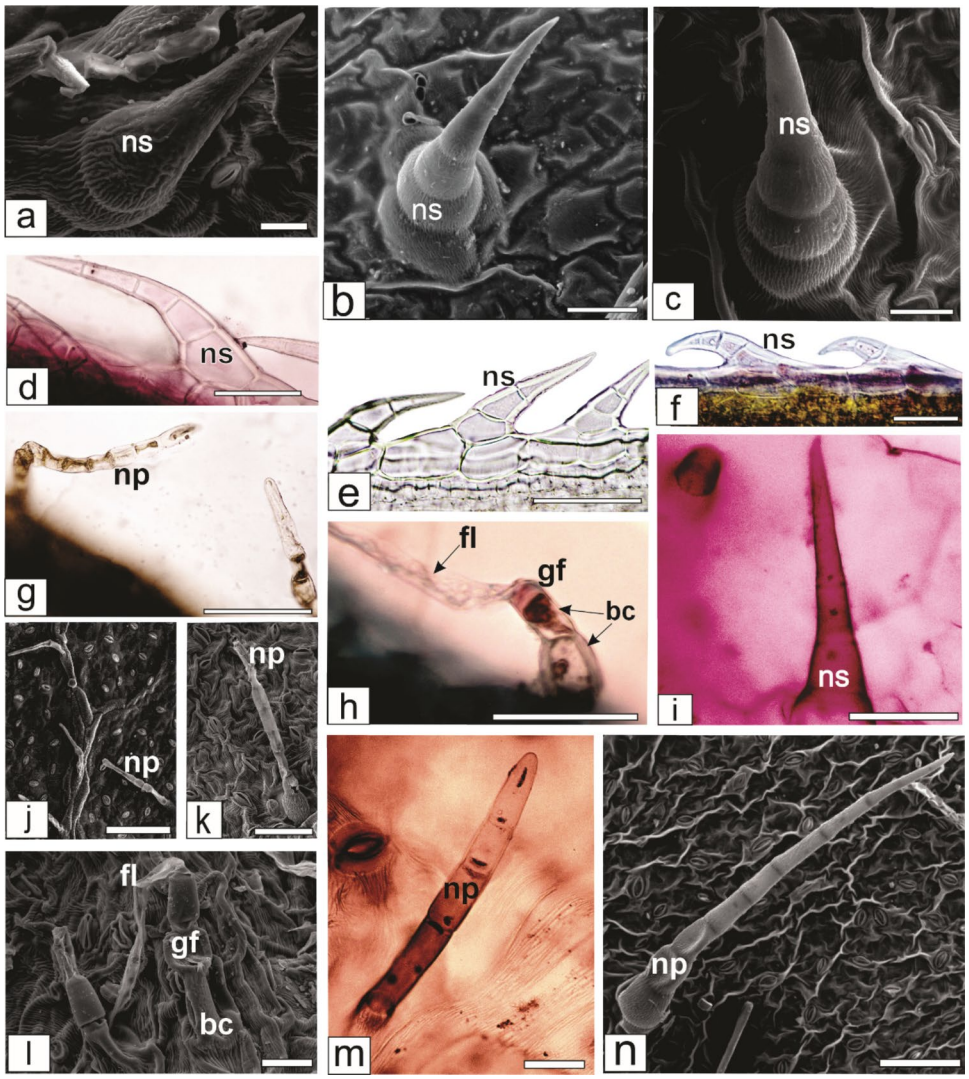

Fig. 3 Leaf trichomes in *Bidens* spp. (**d**–**i**, **m**: light microscopy; **a**–**c**, **j**–**l**, **n**: scanning electron microscopy). *Bidens alba* (**a**, **d**, **g**, **j**–**l**), *B. pilosa* (**b**, **e**, **h**, **m**), *B. subalternans* (**c**, **f**, **i**, **n**) (bc, basal cell; gf, flagelliform glandular trichome (type III); fl, flagellum; ns, unbranched non-glandular trichome (type I); np, pluricellular uniseriate non-glandular trichome (type II)). Scale bar: **a**–**c** = 10 µm, **d**–**l** = 50 µm, **m** = 25 µm, **n** = 100 µm

Results and Discussion

Morphology

In the present study, the key morphological features of the three *Bidens* species are investigated and compared. In general, all three species (Fig. 1a–c) are herbaceous, growing 0.3–1.2 m in height, and share basic morphological features. The stems are green to reddish purple, quadrangular, erect, or decumbent. The leaves are opposite and petiolate. However, the three species have some distinct leaf morphological characteristics that aid in their identification. *Bidens alba* has generally tripartite or pinnatisect leaves, with ovate-lanceolate segments with serrated to deeply toothed margins (Fig. 1a, d), presenting a glabrescent or slightly pubescent indumentum, especially on the veins. In *B. pilosa*, the leaves are pinnatisect to bipinnatisect, with 3 to 5 lanceolate or ovate-lanceolate segments with serrated margins (Fig. 1b, e) and a more evident indumentum, commonly pubescent or strigose on both sides. Whereas, *B. subalternans* is distinguished by its larger leaf division, often bipinnatisect, with narrower ovate-lanceolate segments with deeply serrated margins (Fig. 1c, f) and a predominantly strigose indumentum, giving the blade a rougher texture to the touch.

Also, *B. alba* has inflorescences composed of radiate capitula, being the ray florets white, reflexed, sterile, and measuring 14–16 mm in length; the disc florets are yellow, tubular, fertile, bisexual, and around 5.5 mm long (Fig. 1g); *B. pilosa* possesses inflorescences formed of discoid or radiate capitula, when the ray florets are present are white to salmon-colored, sterile, and approximately 3–4 mm long, while the disc florets are yellow, tubular, and approximately 3.5–4 mm long (Fig. 1h); whereas the inflorescences of *B. subalternans* are composed of discoid or radiate capitula, yellow ray florets, sterile, and 4–6 mm long; yellow disc florets, tubular, and approximately 3–4 mm long (Fig. 1i). These differences, especially the inflorescence, in the degree of leaf division and shape of the segments, and type of

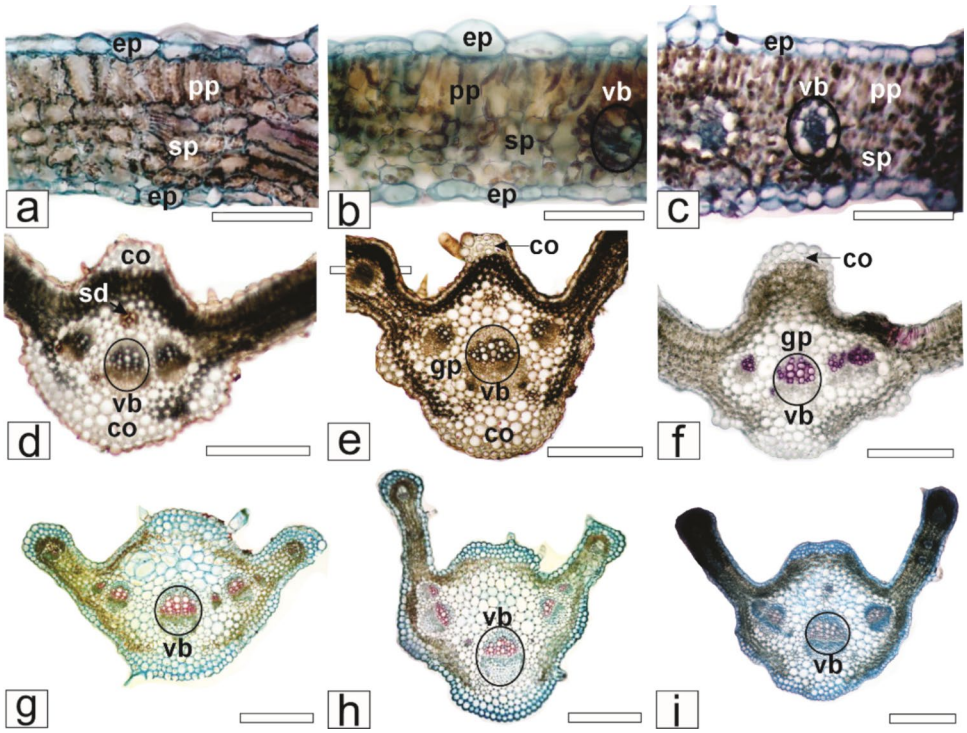

Fig. 4 Leaf anatomy of *Bidens* spp. Cross-section of lamina (**a**–**c**), midrib (**d**–**f**), and petiole (**g**–**i**). *B. alba* (**a**, **d**, **g**), *B. pilosa* (**b**, **e**, **h**), *B. subalternans* (**c**, **f**, **i**) (co, collenchyma; ep, epidermis; gp, ground parenchyma; pp, palisade parenchyma; sd, secretory duct; sp, spongy parenchyma; vb, vascular bundle). Scale bars: **a**–**c** = 50 µm, **d**–**i** = 300 µm

indumentum, are important for the morphological differentiation among these species.

Light Microscopy and Scanning Electron Microscopy

In frontal view, anticlinal epidermal cell walls were classified following the criteria proposed by Yang et al. (2012) as smooth-angled or (slightly) sinuous. They were smooth-angled on both adaxial and abaxial epidermises of *B. alba* (Fig. 2a, d) and sinuous on both surfaces of *B. pilosa* (Fig. 2b, e), whereas *B. subalternans* showed sinuous walls on the adaxial epidermis (Fig. 2c) and slightly sinuous walls on the abaxial epidermis (Fig. 2f). Striate cuticle covers the epidermis in the three studied species (Fig. 2g–l). Also, anomocytic and anisocytic stomata are observed on both sides of the epidermis in the three species, describing the leaf as amphistomatic (Fig. 2a–f). Sinuous anticlinal cell walls, amphistomatic, anomocytic, and anisocytic stomata were also observed in *B. pilosa* by Sa *et al.* (2017). Essiett and Archibong (2014) found diacytic and staurocytic stomata, in addition to anomocytic and anisocytic types, on both leaf surfaces in *B. pilosa* and found brachyparacytic stomata only on the abaxial surface.

Pyramidal crystals (Fig. 2g′) were found on the epidermal cells on the adaxial side, whereas amorphous crystals were observed arising from the stomata (Fig. 2j) on the abaxial side in *B. alba*. The presence of calcium oxalate crystals is a frequent anatomical feature in different plant groups (Raeski et al. 2023), playing functions associated with defense against herbivores, ionic regulation, and calcium storage (Franceschi and Nakata 2005).

The stomata size and the stomatal index have greater taxonomic significance (Cutter 1986). Micro-measurements of stomata show that abaxial leaf surfaces have a higher stomatal index when compared to those of the adaxial sides across all samples. *Bidens alba* (SI = 26.7% adaxial, 43.9% abaxial sides) presents the most distinct difference between adaxial and abaxial sides; *Bidens pilosa* (SI = 33.6% adaxial, 45.7% abaxial sides) evidences the highest average stomatal index on abaxial side, whereas *Bidens subalternans* (SI = 32.7% adaxial, 36.3% abaxial sides) shows the smallest difference between surfaces. Essiett and Archibong (2014) recorded a similar stomatal index for *B. pilosa* with 34% on the adaxial side and 46% on the abaxial side.

Considering the average size of stomata, *B. alba* has abaxial stomata (21 × 15 µm) that are commonly larger than adaxial stomata (18 × 12 µm). However, *B. pilosa* shows the opposite pattern with larger adaxial (18 × 14 µm) than abaxial (17 × 13 µm) stomata. *Bidens subalternans* possesses comparable sizes of stomata on both sides, being 20 × 11 µm on the adaxial side and 19 × 13 µm on the abaxial side. Also, stomata width is more constant than length measurements.

Three types of trichomes were recognized in the present study (Fig. 3a–i). Type I is an unbranched, non-glandular, multicellular uniseriate trichome with a broad base, composed of 4–6 cells with thick walls, and a narrow, elongated apical cell (Fig. 3a–f, i). These trichomes are covered by a striate cuticle (Fig. 3a, c), and tiny crystals are observed

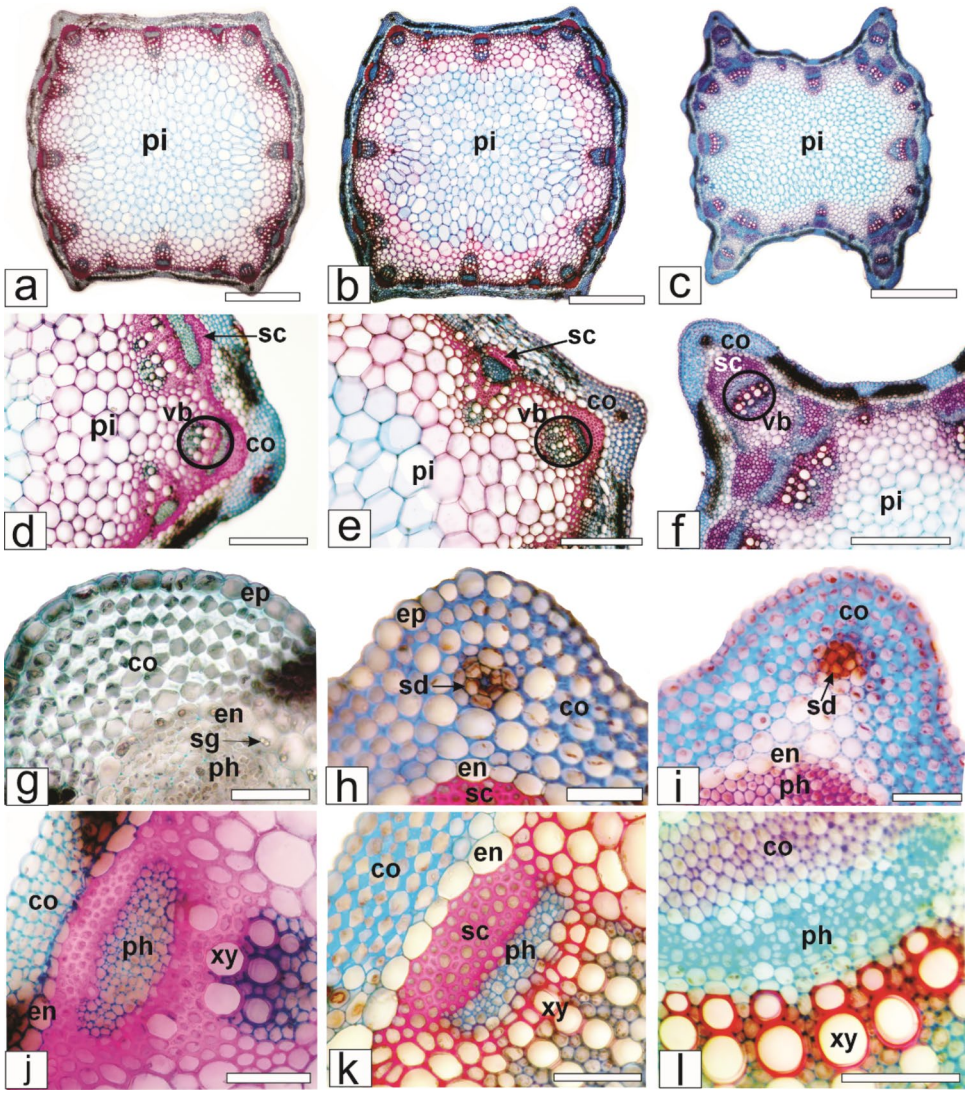

Fig. 5 Anatomy of *Bidens* spp. — stem in cross-section. *B. alba* **a**, **d**, **g**, **j**, *B. pilosa* **b**, **e**, **h**, **k**, *B. subalternans* **c**, **f**, **i**, **l** (co, collenchyma; en, endodermis; ep, epidermis; fi, fiber; ph, phloem; pi, pith; sg, starch grain; sd, secretory duct; vb, vascular bundle; xy, xylem). Scale bars: **a**–**c** = 500 µm, **d**–**f** = 200 µm, **g**–**l** = 50 µm

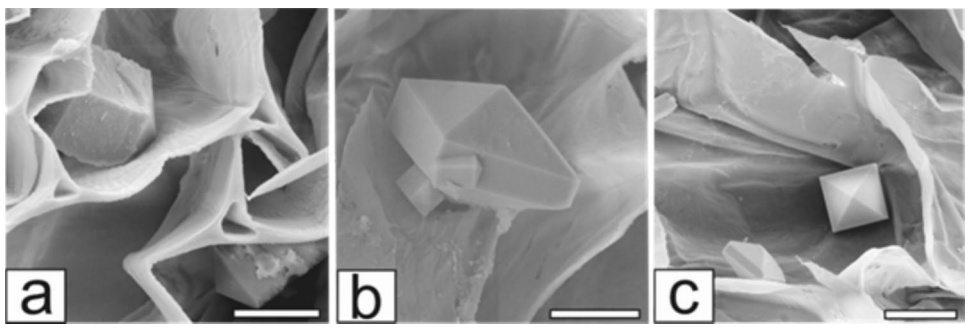

Fig. 6 Scanning electron microscopy of crystals in *Bidens* spp. — stem in cross-section. *B. alba* **a**, *B. pilosa* **b**, *B. subalternans* **c**. Scale bars: **a**, **b** = 10 µm and **c** = 20 µm

inside some cells. The epidermal cells surrounding this trichome are arranged in a rosette pattern. Non-glandular trichomes are also present along the leaf margins, with the apical cells regularly oriented toward the leaf apex in all species (Fig. 3d–f) and make the indument of the leaf strigose.

Type II trichomes are non-glandular, multicellular, uniseriate, formed by 4–10 cells, with the basal cell shaped like a pedestal and covered by striate cuticle, and an apical cell slightly longer than the others (Fig. 3g, j, k, m). This trichome was called by Essiett and Archibong (2014) and Sá

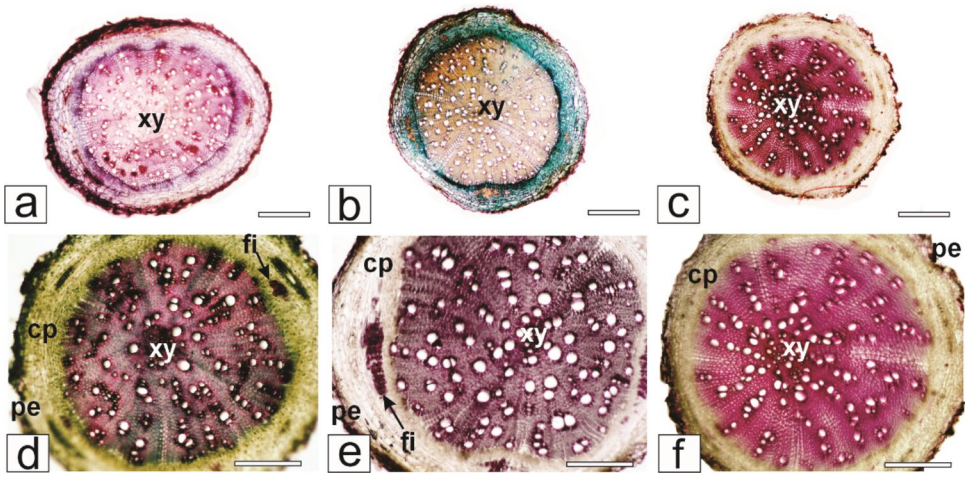

Fig. 7 Anatomy of *Bidens* spp. — root in cross-section. *B. alba* (**a**, **d**), *B. pilosa* (**b**, **e**), *B. subalternans* (**c**, **f**) (co, collenchyma; cp, cortical parenchyma; en, endodermis; fi, fibers; pe, periderm; xy, xylem). Scale bars: **a**–**c** = 500 µm, **d**–**f** = 300 µm

et al. (2017) as glandular. However, no glandular heads or oil production were observed. Type III is a flagelliform glandular trichome (Fig. 3h, l), formed by 1–3 cells at the base and an apical cell from which an elongated, cylindrical tube contains a translucent secretion. *Bidens alba* and *B. pilosa* have all three types of trichomes, whereas *B. subalternans* has only types I and II.

The leaves of all species, in cross-section, present unilayered epidermis covered externally by a moderately thick cuticle that reacts positively with Sudan III. The mesophyll is dorsiventral, comprising one layer of palisade and about four layers of spongy parenchyma. Minor vascular bundles are located in the middle of the mesophyll and are encircled by a parenchyma sheath (Fig. 4a–c). The midrib is biconvex with an angular shape on the adaxial side and a rounded or slightly plane-convex outline on the abaxial side. Trichomes previously described for lamina were also found in the midrib. Beneath the epidermis, one to two layers of angular collenchyma are found on both sides; however, photosynthetic parenchyma is continuous on the adaxial side. The vascular system is represented by three free vascular bundles in an open arc, the central one being larger than the others. Secretory ducts formed by uniseriate epithelium, producing lipophilic material, are found close to the vascular bundles in the ground parenchyma (Fig. 4d–f). The petiole, in cross-section, is biconvex with two wings on the adaxial side (Fig. 4g–i). The overall anatomy of the midrib is similar to that of the petiole.

In cross-section, the stems are quadrangular in shape with four angular projections which may be slightly or deeply prominent in all three species (Fig. 5c, f, i). The epidermis is unilayered, covered by a thin and striated cuticle. In the cortex, chlorenchyma alternates with angular collenchyma (Fig. 5d–f). In the projection regions, various layers of angular collenchyma are observed in the three species (Fig. 5g–i). Secretory ducts are also found in this region (Fig. 5h, i). Idioblasts containing brownish substances corresponding to phenolic compounds are present in the chlorenchyma. Delimiting the cortex, an endodermis is present (Fig. 5g–k), containing starch grains (Fig. 5g) which react positively with iodine solution.

The vascular system of the stem is represented by around 20 vascular bundles forming a ring and delimiting the pith (Fig. 5a–c). There is also a vascular bundle in each projection (Fig. 5c, f). A perivascular fiber cap is found attached to the phloem (Fig. 5). The pith occupies most of the stem's central region and is formed by parenchyma cells (Fig. 5a–c). The three *Bidens* stems showed bipyramidal crystals in the pith (Fig. 6a–c). However, only *B. alba* also displayed cubic crystals in this tissue.

In cross-section, the roots of the three studied species are circular. The development of secondary growth with the presence of periderm can be observed. The cortex is formed by around five layers of parenchyma and encloses secretory ducts. Delimiting the cortex, an endodermis is present and has Casparian stripes. The phloem surrounds the xylem, which occupies the root's central region and shows parenchymatic rays. Groups of fibers are found in the phloem (Fig. 7a–f).

Elemental Analysis of Crystals

The presence of amorphous crystals arising from stomata (Figs. 2j and 8a, b) suggests the existence of an excretion mechanism, probably associated with the elimination of excess calcium or the regulation of osmotic balance, also functioning as a physical barrier against microorganisms and insects. This stomatal phenomenon, although poorly documented, has been associated with the adaptive capacity of certain species to deal with environments rich in mineral salts (Nakata 2015).

After EDS analyses, amorphous crystals showed additional elements, such as potassium, sulfur, and sodium (Fig. 8a, b), whereas the cubic crystal structure was observed when the chemical composition was only calcium oxalate

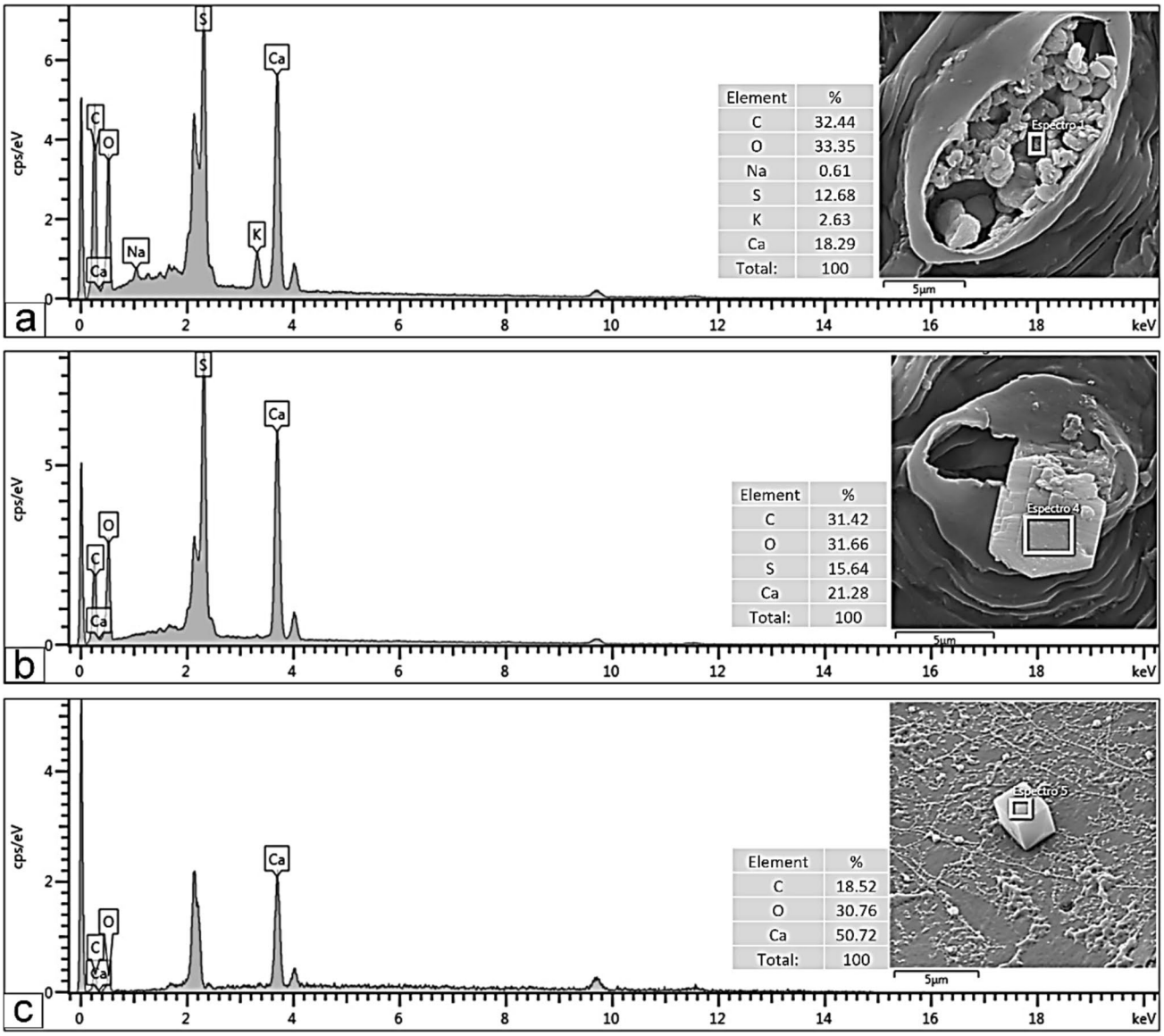

Fig. 8 Field emission scanning electron microscopy image and energy-dispersive X-ray spectroscopy spectra of *Bidens alba*. Amorphous crystal (**a**, **b**) and cubic crystal (**c**). The prominent unlabeled peak at 0 keV is the noise peak, and the peak near 2.1 keV is for gold (Au) used for sputter-coating the samples for SEM analysis

(Fig. 8c). This finding suggests that the incorporation of heterogeneous ions may affect the orderly arrangement of calcium oxalate, leading to changes in crystal morphology.

Chemical Identification Using UPLC-ESI-QTOF

In the present study, LC-MS analysis was employed for the characterization of different compounds tentatively identified in the three species studied divided in stems, roots, and leaves. It showed the presence of polyphenols, including phenolic acids and their derivatives, flavonoids (as well as their glycosidic forms) as the main compounds of the *Bidens* species studied and identified in all plant parts. These molecules have also been previously identified in *Bidens* (Chiang et al. 2004; Silva et al. 2013; Yang 2014; Bartolome et al. 2013; Liang and Xu 2016).

Compounds identified in the three species studied are listed in Table S1. These compounds showed to be similar in all extracts analyzed, with differences in concentration; there were major variations for caffeoylquinic acids, dicaffeoylquinic acids, and some flavonoids such as quercetin and okanin derivatives (Figure S1 and Figure S2). As observable in other species from the genus, phenolic compounds are common in *Bidens* species with the chemical structures and unique characteristics that collectively influence the overall biological activity of the plant.

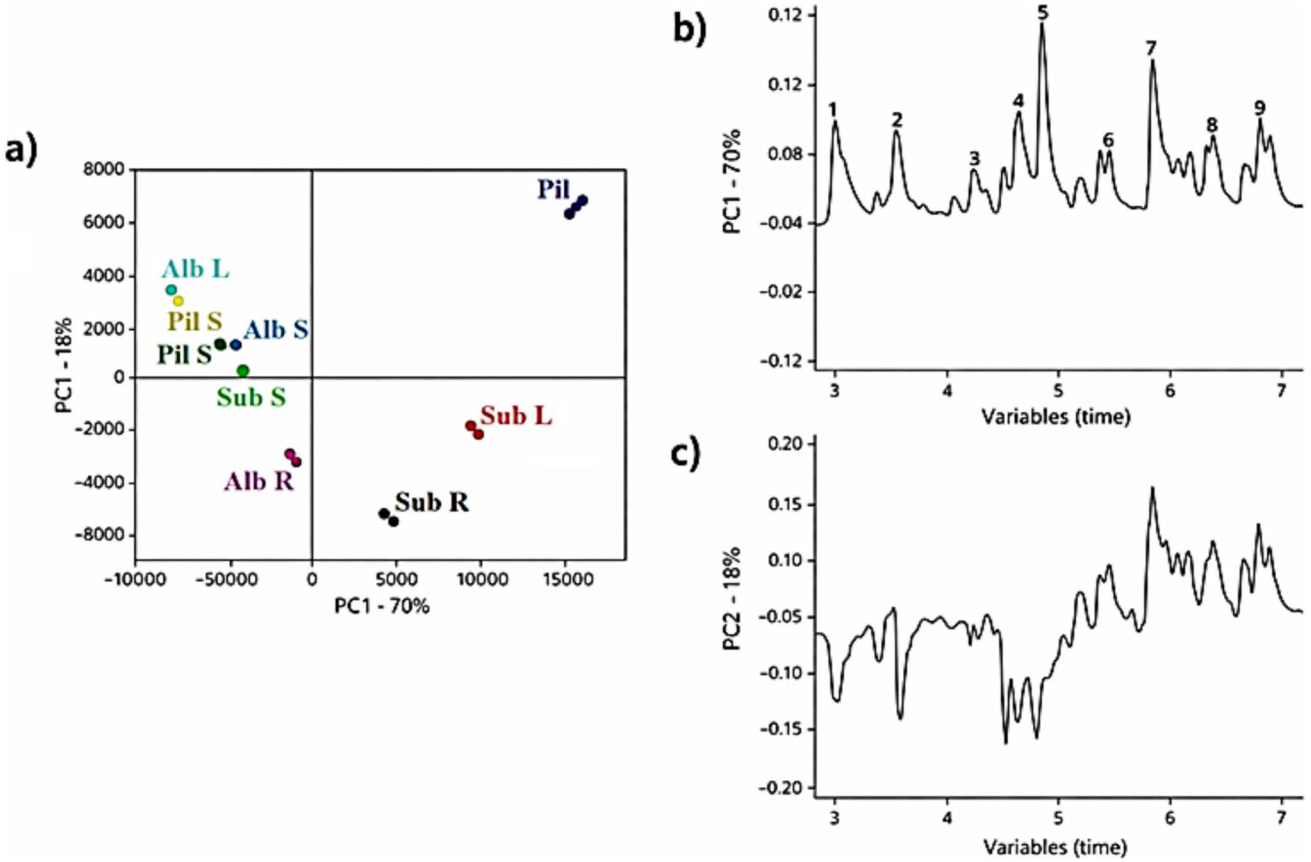

Fig. 9 PC1 × PC2 scores plot on the *Bidens* in different heat times **a**. Loading in line with scores **b** and **c** for PC1 and PC2, respectively. The numbers showed the following identification: 1, 3-*O*-caffeoylquinic acid; 2, caffeoyl-xylose; 3, quercetin-*O*-glucuronide; 4 and 5, di-*O*-caffeoylquinic acid; 6 and 7, okanin-*O*-(diacetyl)-hexoside; 8 and 9, okanin-*O*-(triacetyl)glucoside. The species are described as Alb, *B. alba*; Pil, *B. pilosa*; Sub, *B. subalternans*; L, leaves; R, root; and S, stem

Additionally, as observable in Table S2, 21 compounds were observable and 2 unknowns. Caffeoylquinic and di-*O*-caffeoylquinic acid showed ions at *m/z* 353 and 515; okanin derivatives as ions at *m/z* 533, 575, and 679; quercetin and luteolin derivatives at *m/z* 609, 447, and 531. Other compounds were dihydroxybenzoyl hexoside at *m/z* 315, quinic acid at *m/z* 191, and caffeoyl-xylose at *m/z* 311.

Although the class of samples is known *a priori*, a study based on the unsupervised pattern recognition method was applied to observe the structure of the dataset. The PCA score plot (PC1 × PC2) clearly separates *Bidens* samples according to species, tissue, and heat/steam processing (Fig. 9a). PC1 (70% of the variance) is the main discriminator, distinguishing samples with higher contributions of the markers assigned to peaks 1–9, namely caffeoylquinic acid derivatives (1 and 4–5), caffeoyl-xylose (2), quercetin-*O*-glucuronide (3), and acetylated okanin glycosides (6–9) from samples showing lower relative contribution of these compounds (Fig. 9b). PC2 (18%) further refines the separation by contrasting profiles relatively enriched in the later-eluting acetylated okanin glycosides (6–9; positive PC2 direction) *versus* profiles more associated with the earlier-eluting phenolic markers, especially caffeoylquinic acids and quercetin-*O*-glucuronide (1–5; negative PC2 direction) (Fig. 9c). Overall, the loading plots support that changes in the relative abundance of these phenolic and okanin-derived constituents drive the observed clustering, indicating that both plant matrix (leaves *vs* roots) and processing (steam/heat time) contribute to the chemical differentiation among *Bidens* samples.

To understand the variations of the content, semi-quantification was evaluated by certifying the compounds between the species (Fig. 10a, b) presented high caffeoyl and di-caffeoyl content for *B. subalternans* root and leaves observed in loadings PC1 plot described in positive of PC. Additionally, *B. pilosa* leaves and *B. alba* leaves and root showed variations in caffeoyl and di-caffeoyl (*B. pilosa* leaves showed higher concentrations in both — Fig. 10c), and *B. pilosa* leaves show higher concentration of okanin-*O*-(diacetyl)-hexoside and placed in positive of PC2.

It should be noted that the present study is based on material collected in a single geographic region and during a single

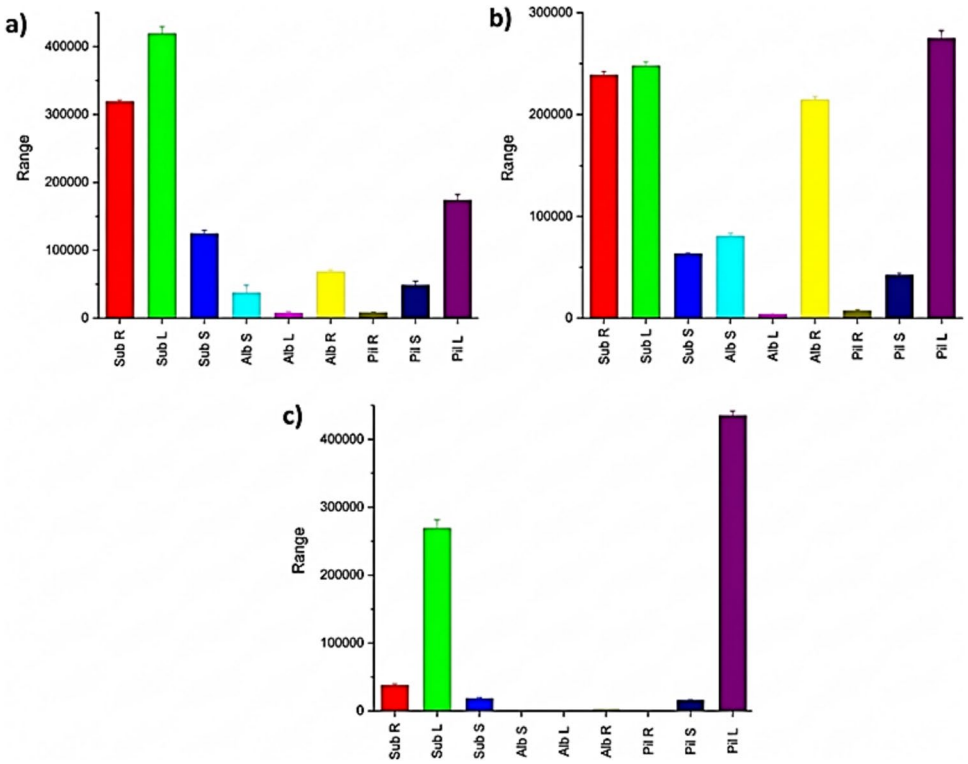

Fig. 10 Bar plot using one-way ANOVA to semi-quantitative (relative peak area) evaluation from caffeoylquinic acid (**a**, compound 4), di-caffeoylquinic acid (**b**, compound 10), and okanin-*O*-(diacetyl)-hexoside (**c**, compound 14) in *Bidens* species: Alb, *B. alba*; Pil, *B. pilosa*; Sub, *B. subalternans*; L, leaf; R, root; S, stem

collection period, with five individuals analyzed per species. Given the high phenotypic plasticity and broad geographic distribution reported for *Bidens* taxa (Grombone-Guaratini et al. 2005), broader sampling across multiple populations, seasons, and environmental conditions would further strengthen the generalization of these diagnostic traits and the associated chemical fingerprints. However, the concordance observed among individuals within each species, together with the complementary evidence provided by morpho-anatomy and LC-MS fingerprinting, supports the consistency of the diagnostic set proposed here for the studied material.

Conclusion

Among the three *Bidens* species studied, morphological identification often leads to confusion. This study demonstrates that the combined use of morpho-anatomical and chemical techniques was decisive for their differentiation.

Certain morpho-anatomical characteristics show potential as reliable markers for species delimitation, particularly inflorescence type, the degree of leaf division, segment shape, indumentum type, the pattern of anticlinal epidermal cell walls, stomatal size and index, trichome assemblages, morphotypes, and crystal composition.

Similarly, chemometric analysis of the species' extract profiles helped reinforce the differences among the three species. Therefore, this combined analytical approach serves as a powerful tool for determining the morpho-anatomical and chemical differences among *B. pilosa*, *B. alba*, and *B. subalternans*, allowing for their clear differentiation.

Overall, this integrated approach provides a useful framework for *Bidens* species authentication and for improving quality control of botanical raw materials. Because the present study is based on material collected in a single region and period ($n = 5$ per species), broader sampling across multiple populations, seasons, and environments will further strengthen the generalization of diagnostic traits and chemical fingerprints and support extension of this strategy to additional taxa within the *B. pilosa* complex.

Supplementary Information The online version contains supplementary material available at https://doi.org/10.1007/s43450-026-00759-8.

Author Contribution CS, IS, ACTV: methodology, investigation, data curation; JM, FLB: writing, review and editing; IPM: investigation, resources (plant material); LSC: investigation, data curation; PVF: editing; CAM, VR: botanical identification; FLB, ESB, PRVR: data curation, chemical analysis, writing original draft; JM: microscopic analysis supervision, writing original draft. All authors approved the final version of the manuscript.

Funding The Article Processing Charge (APC) for the publication of this research was funded by the Coordenação de Aperfeiçoamento de Pessoal de Nível Superior - Brasil (CAPES) (ROR identifier: 00x0ma614). This research was funded by CAPES–Coordenação de Aperfeiçoamento de Pessoal de Nível Superior, scholarships numbers (88887.977850/2024-00; 88887.974351/2024-00) and UEPG–Universidade Estadual de Ponta Grossa.

Data Availability The datasets used during the current study are available from the corresponding author on reasonable request.

Declarations

Ethics Approval Access to the plant material is authorized by CGEN/SISGEN under code A1E6FA8.

Competing Interests The authors declare no competing interests.

References

Antunes KA, Raman V, Perera WH, Heiden G, Pontarolo R, Farago PV, Khan IA, Manfron J (2024) Authentication and quality control of the Brazilian traditional herb 'carquejas' (*Baccharis* species) using morpho-anatomy and microscopy. Plants 13:3030. https://doi.org/10.3390/plants13213030

Bartolome AP, Villaseñor IM, Yang WC (2013) *Bidens pilosa* L. (Asteraceae): botanical properties, traditional uses, phytochemistry, and pharmacology. Evid Based Complement Alternat Med 2013:340215. https://doi.org/10.1155/2013/340215

Berlyn GP, Miksche JP (1976) Botanical Microtechnique and Cytochemistry. Iowa State University Press, Ames, Iowa

Borges CC, Matos TF, Moreira J, Rossato AE, Zanette VC, Amaral PA (2013) *Bidens pilosa* L. (Asteraceae): traditional use in a community of southern Brazil. Rev Bras Plantas Med 15:34–40. https://doi.org/10.1590/S1516-05722013000100004

Bringel Jr JBA, Reis-Silva GA, Barbosa ML (2025) *Bidens*. Flora e Funga do Brasil. Jardim Botânico do Rio de Janeiro. Available from: https://floradobrasil.jbrj.gov.br/FB103747. Accessed 18 March 2025

Chagas-Paula DA, Zhang T, Da Costa FB, Edrada-Ebel R (2015) A metabolomic approach to target compounds from the Asteraceae family for dual COX and LOX inhibition. Metabolites 5:404–430. https://doi.org/10.3390/metabo5030404

Chen Y, Luo J, Zhang Q, Kong L (2016) Identification of active substances for dually modulating the renin–angiotensin system in *Bidens pilosa* by liquid chromatography–mass spectrometry–based chemometrics. J Funct Foods 21:201–211. https://doi.org/10.1016/j.jff.2015.12.028

Chiang YM, Chuang DY, Wang SY, Kuo YH, Tsai PW, Shyur LF (2004) Metabolite profiling and chemopreventive bioactivity of plant extracts from *Bidens pilosa*. J Ethnopharmacol 95:409–419. https://doi.org/10.1016/j.jep.2004.08.010

Cortés-Rojas DF, Chagas-Paula DA, Da Costa FB, Souza CRF, Oliveira WP (2013) Bioactive compounds in *Bidens pilosa* L. populations: a key step in the standardization of phytopharmaceutical preparations. Rev Bras Farmacogn 23:28–35. https://doi.org/10.1590/S0102-695X2012005000100

Cutter EG (1986) Anatomia vegetal: parte I – células e tecidos. Roca, São Paulo

Duarte MR, Estelita MEM (1999) Caracteres anatômicos de *Bidens pilosa* L., Asteraceae. Hoehnea 26:15–27

Essiett UA, Archibong IA (2014) The taxonomic significance of certain anatomical variation in four genera of Asteraceae. Bull Environ Pharmacol Life Sci 3:150–163

Foster AS (1949) Practical plant anatomy. D. Van Nostrand Company, Princeton

Franceschi VR, Nakata PA (2005) Calcium oxalate in plants: formation and function. Annu Rev Plant Biol 56:41–71. https://doi.org/10.1146/annurev.arplant.56.032604.144106

Fuchs CH (1963) Fuchsin staining with NaOH clearing for lignified elements of whole plants or plant organs. Stain Technol 38:141–144. https://doi.org/10.3109/10520296309067156

Gabe M (1968) Techniques histologiques. Masson et Cie, Paris

Gbashi S, Njobeh P, Steenkamp P, Madala N (2017) Pressurized hot water extraction and chemometric fingerprinting of flavonoids from *Bidens pilosa* by UPLC-tandem mass spectrometry. CyTA J Food 15:171–180. https://doi.org/10.1080/19476337.2016.1230151

Gempo N, Yeshi K, Jamtsho T, Jamtsho L, Samten, Wangchuk P (2024) Development of quality control parameters for two Bhutanese medicinal plants (*Aster flaccidus* Bunge and *Aster diplostephioides* (DC.) Benth. ex C.B.Clarke) using traditional and modern pharmacognostical platforms. Heliyon 10:e24969. https://doi.org/10.1016/j.heliyon.2024.e24969

Gilbert B, Alves LF, Favoreto R (2013) *Bidens pilosa* L. Asteraceae (Compositae; subfamília Heliantheae). Rev Fitos 8:53–67. https://doi.org/10.32712/2446-4775.2013.194

Grombone-Guaratini MT, Solferini VN, Semir J (2004) Reproductive biology in species of *Bidens* L. (Asteraceae). Scientia Agricola 61:185–189. https://doi.org/10.1590/S0103-90162004000200010

Grombone-Guaratini MT, Silva-Brandão KL, Solferini VN, Semir J, Trigo JR (2005) Sesquiterpene and polyacetylene profile of the *Bidens pilosa* complex (Asteraceae: Heliantheae) from Southeast of Brazil. Biochem Syst Ecol 33:479–486. https://doi.org/10.1016/j.bse.2004.11.005

Grombone-Guaratini MT, Mansanares ME, Semir J, Solferini VN (2006) Chromosomal studies of three species of *Bidens* (L.) (Asteraceae). Caryologia 59:14–18. https://doi.org/10.1080/00087114.2006.10797892

Johansen DA (1940) Plant Microtechnique. McGraw-Hill Book Company, New York and London

Khoza BS, Gbashi S, Steenkamp PA, Njobeh PB, Madala NE (2016) Identification of hydroxylcinnamoyl tartaric acid esters in *Bidens pilosa* by UPLC-tandem mass spectrometry. S Afr J Bot 103:95–100. https://doi.org/10.1016/j.sajb.2015.08.018

Lans CA (2006) Ethnomedicines used in Trinidad and Tobago for urinary problems and diabetes mellitus. J Ethnobiol Ethnomed 2:45. https://doi.org/10.1186/1746-4269-2-45

Liang X, Xu Q (2016) Separation and identification of phenolic compounds in *Bidens pilosa* by ultra-high performance liquid chromatography with quadrupole time-of-flight mass spectrometry. J Sep Sci 39:1853–1862. https://doi.org/10.1002/jssc.201600017

Lorenzi H, Matos FJA (2008) Plantas medicinais no Brasil: nativas e exóticas, 2nd ed. Instituto Plantarum, Nova Odessa

Lusa MG, Martucci MEP, Loeuille BFP, Gobbo-Neto L, Appezzato-da-Glória B, Da Costa FB (2016) Characterization and evolution of secondary metabolites in Brazilian Vernonieae (Asteraceae) assessed by LC-MS fingerprinting. Bot J Linn Soc 182:594–611. https://doi.org/10.1111/boj.12480

Machinski I, Andrade EA, Schaffka VM, Almeida VP, Santos A, Bueno D, Perera WH, Pereira RP, Manfron J, Miyoshi E, Beltrame FL (2024) Exploring the pharmacognostical and phytochemical

profiles of aqueous extracts of *Kalanchoe*. Chem Biodivers 21:e202400660. https://doi.org/10.1002/cbdv.202400660

Miosic S, Knop K, Hölscher D, Greiner J, Gosch C, Thill J, Kai M, Shrestha BK, Schneider B, Crecelius AC, Schubert US, Svatoš A, Stich K, Halbwirth H (2013) 4-Deoxyaurone formation in *Bidens ferulifolia* (Jacq.) DC. PLoS One 8:e61766. https://doi.org/10.1371/journal.pone.0061766

Nakata PA (2015) An assessment of engineered calcium oxalate crystal formation on plant growth and development as a step toward evaluating its use to enhance plant defense. PLoS One 10:e0141982. https://doi.org/10.1371/journal.pone.0141982

Ong PL, Weng BC, Lu FJ, Lin ML, Chang TT, Hung RP, Chen CH (2008) The anticancer effect of protein extract from *Bidens alba* in human colorectal carcinoma SW480 cells. Food Chem Toxicol 46:1535–1547. https://doi.org/10.1016/j.fct.2007.12.015

Ortega CA, María AOM, Gianello JC (2000) Chemical components and biological activity of *Bidens subalternans*, *B. aurea* (Asteraceae) and *Zuccagnia punctata* (Fabaceae). Molecules 5:465–467. https://doi.org/10.3390/50300465

POWO (2025) Plants of the World Online. Royal Botanic Gardens, Kew. Available from: https://powo.science.kew.org. Accessed 18 March 2025

Raeski PA, Heiden G, Novatski A, Raman V, Khan IA, Manfron J (2023) Calcium oxalate crystal macropattern and its usefulness in the taxonomy of *Baccharis* (Asteraceae). Microsc Res Tech 86:862–881. https://doi.org/10.1002/jemt.24363

Ramabulana A-T, Steenkamp P, Madala N, Dubery IA (2020) Profiling of chlorogenic acids from *Bidens pilosa* and differentiation of closely related positional isomers with the aid of UHPLC-QTOF-MS/MS-based in-source collision-induced dissociation. Metabolites 10:178. https://doi.org/10.3390/metabo10050178

Roeser KR (1972) Die Nadel der Schwarzkiefer – Massenprodukt und Kunstwerk der Natur. Mikrokosmos 61:33–36

Sá RD, Silva FR, Randau KP (2017) Pharmacobotanical characterization of *Bidens pilosa* L. J Environ Anal Progr 2:349–357. https://doi.org/10.24221/jeap.2.3.2017.1375.349-357

Safer S, Cicek SS, Pieri V, Schwaiger S, Schneider P, Wissemann V, Stuppner H (2011) Metabolic fingerprinting of *Leontopodium* species (Asteraceae) by means of 1H NMR and HPLC–ESI-MS. Phytochemistry 72:1379–1389. https://doi.org/10.1016/j.phytochem.2011.04.006

Saltos MBV, Naranjo Puente BFN, Milella L, De Tommasi N, Braca A (2015) Antioxidant and free radical scavenging activity of phenolics from *Bidens humilis*. Planta Med 81:1056–1064. https://doi.org/10.1055/s-0035-1545928

Sass JE (1951) Response of meristems of seedlings to benzene hexachloride used as a seed protectant. Science 114:466. https://doi.org/10.1126/science.114.2966.466

Silva DB, Okano LT, Lopes NP, de Oliveira DCR (2013) Flavanone glycosides from *Bidens gardneri* Bak. (Asteraceae). Phytochemistry 96:418–422. https://doi.org/10.1016/j.phytochem.2013.09.024

Yang WC (2014) Botanical, pharmacological, phytochemical, and toxicological aspects of the antidiabetic plant *Bidens pilosa* L. Evid Based Complement Alternat Med 2014:698617. https://doi.org/10.1155/2014/698617

Yang Y, Zhang LY, Liu B, van der Werff H (2012) Leaf cuticular anatomy and taxonomy of *Syndiclis* (Lauraceae) and its allies. Syst Bot 37:861–878. https://doi.org/10.1600/036364412X656518